

A Numerical Model for Predicting the Radial Power Profile in CANDU-PHWR Fuel Pellet

Woan Hwang and Ho Chun Suk

Korea Atomic Energy Research Institute

Won Mok Jae

Hanyang University

(received April 30, 1991)

CANDU-PHWR 핵연료 소결체의 반경방향 출력분포 수치모형

황 완 · 석호천

한국원자력연구소

제원목

한양대학교

(1991, 4, 30 접수)

Abstract

An accurate and fast running NEDAR model for calculating radial power profile throughout fuel life in both solid and annular pellets for existing and advanced CANDU-PHWR-fuel was developed in this work. This model contains resultant flux depression equations and neutron depression data tables which have been developed for CANDU-PHWR fuel of pellet with the diameter 8.0 to 19.5 mm and enrichment 0.71–6.0 wt % U-235, over a burnup range of 0 to 840 MWh/kgU (35000 MWD/T). In order to obtain the neutron flux distribution in the fuel pellet, the CE-HAMMER physics code was run for a neutron flux spectrum appropriate to a CANDU-PHWR to give predictions of radial power profile for several ranges of fuel design parameters. The results, which were calculated by the CE-HAMMER physics code, were fitted to an equation which is solved in terms of Bessel and exponential functions in order to obtain the parameters, κ , β and λ in the resultant equation.

The present NEDAR model produce a radial profile which, when normalized to unity at the pellet surface, is slightly higher than the profile of the original ELESIM data table. The predictions of the fission gas release by KAFEP-NEDAR are in slightly better agreement with the experiments than those of ELESIM. The NEDAR model described in this study has been shown to provide an effective, reliable, and accurate method for determining radial power profiles in CANDU-PHWR fuel rods without incurring a significant increase in computing time.

요 약

본 연구에서는 CANDU-PHWR 형 기존 및 개량 핵연료의 원통형(solid) 및 환상형 소결체에 대하여, 그 핵연료 전 수명 기간동안, 반경방향 출력분포를 정확하고 신속하게 계산하는 NEDAR 모

형을 개발하였다. 본 계산모형에는 핵연료소결체의 직경 범위 8.0–19.5 mm, 농축도 범위 0.71–6.0 wt % U-235이고, 계산 가능 연소도범위가 0–840 MWh/kgU (35000MWD/T)인 한계내에서, 핵연료 반경방향 출력분포결과식 및 열중성자속감소 계산결과자료가 포함되어 있다. CANDU-PHWR 형 원자로 중성자속 스펙트럼을 입력자료로 하여, 로물리 전산코드, CE-HAMMER를 이용하여 핵연료의 각 설계조건 및 소결체의 환별 국부지점에 대하여, 임의로 설정한 기준 연소시점에서 반경 방향 출력 분포를 계산하였다. 이 계산 결과를 토대로 각 환의 평균출력을 구하는 적분법 및 비선형 곡선회귀계산법에 의하여, Bessel 함수와 지수함수의 다항식으로 구성된 반경방향 출력분포 기본 결과식 및 그 계수들이 산출되었다.

본 연구에서 개발된 NEDAR 모형을 이용하여 산출한 반경방향출력분포값을, 핵연료소결체 표면에서의 값을 기본단위로 환산하여 비교하면, 본 모형에 의한 반경방향 출력분포 결과가 기존 ELESIM 전산코드의 결과에 비교하여 약간 높게 나타났다. 소결체의 반경방향의 출력 및 온도분포는 핵분열기체생성물방출과 밀접한 관계가 있으므로, 본 모형을 기존 ELESIM 전산코드의 반경방향 출력분포 계산 모형과 대체한 전산코드, 즉 KAFEP-NEDAR에 의한 핵분열기체생성물방출량 예측치를 기존 ELESIM 전산코드의 예측치와 비교하였다. 여기서 KAFEP-NEDAR의 예측치가 실험결과 자료에 보다 더 가깝게 접근하였다. 따라서, 본 연구에서 개발된 NEDAR 모형은 과대한 계산시간의 낭비없이 CANDU-PHWR 형 핵연료소결체의 반경방향출력분포를 효율적이고, 신속/정확하게 계산하는 모형임이 입증되었다.

Nomenclature

$\phi(0)$ =constant (neutron flux at the centre, No.of neutrons/cm²–sec)

$\phi(r)$ =neutron flux at radius r (No. of neutrons/cm²–sec)

$h(r)$ =heat generation rate at radius r (W/m³)

$h(0)$ =heat generation rate at the centre (W/m³)

κ =neutron inverse diffusion length (1/mm)

r =coordinate in radial direction (mm)

a =radius of pellet (mm)

b =radius of pellet central hole (mm)

β, λ =empirical parameters in the flux depression term

I_0 =zero-order modified Bessel function of first kind

I_1 =first-order modified Bessel function of first kind

K_0 =zero-order modified Bessel function of second kind

K_1 =first-order modified Bessel function of second kind

k =thermal conductivity (kW/m.K)

T =temperature (°C)

q' =linear power (kW/m)

h =heat generation rate per unit volume (W/m³)

1. Introduction

The variation of the radial power profile with

burnup in a fuel pellet is a complicated function both of pellet design parameters, such as geometry and initial enrichment, and of reactor operating conditions. The fuel performance analysis code for

CANDU-PHWR, ELESIM⁽¹⁾, uses a fast running method for neutron flux depression model in which the applicable fuel-diameter and burnup range are 12.15 to 19.5 mm and 0 to 480 MWh/kgU, respectively. Also, there are some deviations in the radial power profile of fuel pellet. The purpose of this study is to provide a simple method to accurately predict the radial power distribution and a database for neutron flux depression parameters capable of being used in a long range of burnup and wide range of pellet diameter for advanced fuel design.

In this study an accurate and fast running NEDAR (NEutron Depression Analysis Routine) model for calculating radial power profile throughout fuel life in both solid and annular fuel pellets for CANDU type reactor has been developed. This model contains resultant flux depression equation and neutron depression tables which have been developed for CANDU-PHW type reactor fuel of pellet diameter 8.0 to 19.5 mm and enrichment 0.71–6.0 wt % U-235, over a burnup range of 0 to 840 MWh/kgU (35000 MWd/t). In the NEDAR model described here an approximation to this complex variation has been formulated using a simple model and economical computer routines which are sufficiently physically based so as to be capable of being applied reliably to the fuel design, utilized in CANDU-PHWR type of thermal reactor.

It is frequently assumed that the rate of thermal power generation across a fuel element is essentially constant. This assumption is reasonably valid in fast reactors but less accurate in thermal reactors⁽²⁾. Also, this assumption may provide a satisfactory radial profile in the early stages of the fuel life, but little or no attempt has been made to modify its shape as burnup proceeds. The thermal flux originates outside the fuel element in the moderator. Hence, the flux decreases as one moves towards the center of the fuel due to neutron absorption in the fuel. As irradiation proceeds

the original fissile atoms are depleted in the fuel, fission products build up and new fissile atoms are formed. Since these processes are dependent on the neutron flux level and spectrum, the local fission rate within the fuel pellet will vary with burnup. The Pu-239 formed in UO₂ pellet during irradiation in thermal reactors is nonuniformly distributed. The radial distribution of plutonium formed by thermal neutron capture is governed by the radial thermal neutron flux distribution in the fuel⁽³⁾. In practice, the build up of plutonium atoms near the fuel surface has the greatest effect on the CANDU-PHWR fuel, which is used natural uranium, and produces higher fission rates at the surface as burnup proceeds. To approximate these effects, equations (2.1) and (2.3) in section 2 are adopted.

For fuel performance analysis codes in general, a model of the radial power profile is required in order that the temperature distribution within the fuel may be determined accurately without incurring a significant increase in computing time. In order to obtain the neutron flux distribution in the fuel pellet, the CE-HAMMER physics code⁽⁴⁾ was run for a neutron flux spectrum appropriate to a CANDU power reactor to give predictions of radial power profile for several ranges of fuel design parameters. The results calculated by the CE-HAMMER physics code were fitted to an equation which was solved in terms of Bessel and exponential functions by a non-linear curve fitting subroutine, NL2INT⁽⁵⁾.

The resultant flux depression equations and neutron flux depression database have been incorporated as subroutines into the CANDU-PHWR type fuel performance analysis code, KAFEP⁽⁶⁾. This updated code is referred to as KAFEP-NEDAR hereafter. The model's predictions have been verified for several cases of pellet conditions by comparing them with the experiments.

2. Theory of Neutron Depression in Fuel Element

2.1 The Solution of the Resulting Diffusion Equations

The flux profile is the solution of the resulting diffusion equations which are solved in terms of modified Bessel functions, I and K , and exponential function. The solutions take on different forms according to whether the pellet is solid or hollow.

2.1.1 The Radial Flux Distribution in a Solid Cylindrical Fuel

Appreciable neutron flux depression expressed by^(7,8)

$$\phi_1 = \phi_0 \{I_0(\kappa r) + \beta \exp(\lambda(r-a))\} \quad (2.1)$$

Since the rate of heat generation, h_r , in radius r is proportional to the neutron flux

$$h_r = h_0 \{I_0(\kappa r) + \beta \exp(\lambda(r-a))\} \quad (2.2)$$

2.1.2 The Radial Flux Distribution in an Annular Fuel

Appreciable neutron flux depression expressed by^(7,8)

$$\phi_r = \phi_0 \left\{ I_0(\kappa r) - \frac{I_1(\kappa b)}{K_1(\kappa b)} \left[K_0(\kappa r) + \beta \exp(\lambda(r-a)) \right] \right\} \quad (2.3)$$

Since the rate of heat generation, h_r , in radius r is proportional to the neutron flux

$$h_r = h_0 \left\{ I_0(\kappa r) + \frac{I_1(\kappa b)}{K_1(\kappa b)} \left[K_0(\kappa r) + \beta \exp(\lambda(r-a)) \right] \right\} \quad (2.4)$$

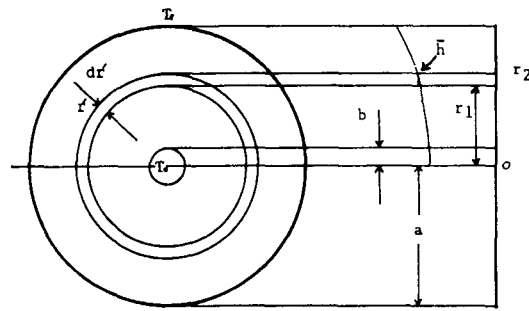
2.2 The Energy Equation for a Cylindrical Pellet

The energy equation for a cylindrical pellet with internal heat generation is⁽⁷⁾:

$$\frac{d}{dr} \left(kr \frac{dT}{dr} \right) + h_r r = 0 \quad (2.5)$$

where, $h_r = h_0 \left\{ I_0(\kappa r) + \frac{I_1(\kappa b)}{K_1(\kappa b)} \right.$

$$\left. K_0(\kappa r) + \beta \exp(\lambda(r-a)) \right\}$$



And the boundary conditions are

$$i) \left. \frac{dT}{dr} \right|_{r=b} = 0; \text{ i.e., no heat transfer through the inner surface}$$

$$ii) T(r=a) = T_s$$

Integrating equation (2.5) from b to a radius inside the pellet, and using the boundary conditions i) and ii):

$$kr \frac{dT}{dr} \Big|_b + \int_b^r (h_r r) dr = 0 \quad (2.6)$$

This equation can now be written in finite difference form with the temperature node at the inner surface of annulus i . Assuming a linear temperature distribution T_i the annulus i with the thickness Δr , the temperature gradient can be approximated by

$$\frac{T_{r+1} + T_i}{\Delta r} \quad (2.7)$$

However, use of linear distribution requires a very large number of steps in the r direction (i.e., many annuli). If a parabolic temperature distribu-

tion is assumed, the temperature distribution can be expressed by

$$T(r) = A - B r^2 \quad (2.8)$$

where A and B are constant.

The gradient is

$$\frac{dT}{dr} = -2 B r \quad (2.9)$$

but at $T_i = A - B r_i^2$ at $r = r_i$

$$T_{i+1} = A - B r_{i+1}^2 \text{ at } r = r_{i+1}$$

solving for B, B is

$$\frac{T_{i+1} - T_i}{r_{i+1}^2 - r_i^2} = -B \quad (2.10)$$

Substituting equation (2.10) into (2.9), the gradient is given to

$$\frac{dT}{dr} = 2 \frac{T_{i+1} - T_i}{r_{i+1}^2 - r_i^2} r = 2 \frac{(T_{i+1} - T_i) r}{(r_{i+1} - r_i)(r_{i+1} + r_i)}$$

but in the case of $r_{i+1} = r_i + \Delta r$, the gradient becomes

$$\begin{aligned} \frac{dT}{dr} &= 2 \frac{T_{i+1} - T_i}{\Delta r (r_{i+1} + r_i)} r \\ \frac{dT}{dr} \Big|_{r=r_i} &= \frac{1}{\Delta r} (T_{i+1} - T_i) \frac{2r_i}{r_{i+1} + r_i} \end{aligned} \quad (2.11)$$

Thus, equation (2.6) becomes, in finite difference form :

$$k_{i+1} r_i \frac{(T_{i+1} - T_i) \cdot 2r_i}{\Delta r (r_{i+1} + r_i)} + \int_b^{r_i} (h_r \cdot r) dr = 0 \quad (2.12)$$

where $k_{i+1} = k(T_{i+1})$

Equation (2.12) can be solved with respect to T_i :

$$T_i = T_{i+1} + \frac{(r_{i+1} + r_i) \cdot \Delta r}{2r_i (k_{i+1} \cdot r_i)} \int_b^{r_i} (h_r \cdot r) dr \quad (2.13)$$

And performing the integration, T_i is given by

$$\begin{aligned} T_i &= T_{i+1} + \frac{(r_{i+1} + r_i) \cdot \Delta r}{2r_i k_{i+1} r_i} h \left\{ \frac{1}{\kappa} [r_i I_1(\kappa r_i) \right. \\ &\quad \left. - b I_1(b) - \frac{I_1(\kappa b)}{K_1(\kappa b)} [r_i K_1(\kappa r_i) - b K_1(\kappa b)] \right\} \\ &\quad + \frac{\beta}{\lambda^2} e^{-\lambda a} \left\{ e^{\lambda r_i} (\lambda r_i - 1) - e^{\lambda b} (\lambda b - 1) \right\} \end{aligned} \quad (2.14)$$

for $b=0$ (no central hole)

$$\begin{aligned} T_i &= T_{i+1} + \frac{(r_{i+1} + r_i) \cdot \Delta r}{2r_i (k_{i+1} \cdot r_i)} \left\{ \frac{r_i I_1(\kappa r_i)}{\kappa} \right. \\ &\quad \left. + \frac{\beta}{\lambda^2} e^{\lambda a} \left\{ e^{\lambda r_i} (\lambda r_i - 1) + 1 \right\} \right\} \end{aligned} \quad (2.15)$$

Hence, the implicit function of equations (2.14) and (2.15) can be expressed as follows ;

$$\begin{aligned} T_i &= T_{i+1} + \Delta T \\ &= T_{i+1} + f(q', \kappa, \beta, \lambda, a, b) \end{aligned} \quad (2.16)$$

where, the parameters of κ , β and λ are calculated by using the methods in Section 3.

3. The Calculational Methods and Application

3.1 The CE-HAMMER Physics Code and Its Input Data

The CE-HAMMER system physics code is a heterogeneous lattice analysis code with depletion using heterogeneous analysis by the multigroup method of exponentials. The input data for the CE-HAMMER physics code were obtained from references (4) and (9). The important input parameters and data for CE-HAMMER are as follows.

3.1.1 Isotope Composition and Concentration, and Others

Concentrations for enrichments of 0.71, 1.0, 1.5, 2.0, 3.0 and 6.0 wt % U-235 are shown in Table 3.1. This table was made by assuming that all fuel has a standard CANDU-PHWR fuel density, 10.64 g/cm³. To a first order, values of κ and λ are proportional to fuel density.

The mesh points and boundary condition used in this analysis are as follows :

- mesh No. in pellet : 10
- mesh No. in moderate : 8
- boundary condition in outer boundary : net zero current

3.1.2 Effective Neutron Temperature

The addition of a neutron absorber(or leakage) to a reactor system tends to shift the equilibrium neutron spectrum to higher (or lower) energies, much as would occur if one were to change the temperature characterizing the Maxwell-Boltzman neutron distribution^(10,11,12).

In this study, the effective neutron temperature was obtained from the output of LATREP⁽¹³⁾ code directly. The average effective neutron temperature varied with the 6 enrichments used and is shown in Table 3.2.

3.1.3 Material Buckling

If it is assumed that a nuclear reactor is operated at a constant power level, then the fission chain reaction is in steady state (e.g. critical).

According to the references^(9,10,14),

B_m^2 depends only on the material composition of the reactor core (whereas B_g^2 depends only on the core geometry), our criticality conditions can be written very concisely as⁽¹⁰⁾

$$B_m^2 = B_g^2$$

If the geometric condition is specified, one can compute the geometric buckling B_g^2 . According to the reference (9), B_g^2 is 0.7891 [cm^{-2}] for a Canadian Bruce type reactor.

3.2 The Calculational Methods Using the Output of the CE-HAMMER Physics Code

From the foregoing description in Section 2, it follows that the ratio of the local fission rate $h(r)$ at radius r to the fission rate at the fuel centre $h(0)$ is assumed to vary as

$$h(r) = h(0) [I_0(\kappa r) + \beta \exp(\lambda(r-a))] \quad (3.0)$$

Table 3.1 Isotope Density

ENRICHMENT	ISOTOPE			
	U-235	U-236	U-238	O-32
0.71	1.685×10^{-4}	1.000×10^{-15}	2.356×10^{-2}	4.746×10^{-2}
1.0	2.373×10^{-4}	1.000×10^{-15}	2.349×10^{-2}	4.746×10^{-2}
1.5	3.559×10^{-4}	1.000×10^{-15}	2.337×10^{-2}	4.746×10^{-2}
2.0	4.746×10^{-4}	1.000×10^{-15}	2.325×10^{-2}	4.746×10^{-2}
3.0	7.119×10^{-4}	1.000×10^{-15}	2.302×10^{-2}	4.746×10^{-2}
6.0	1.424×10^{-4}	1.000×10^{-15}	2.231×10^{-2}	4.746×10^{-2}

NOTE : 1) isotope unit ; atoms / (cm^3) = 10^{24}
enrichment ; wt % U-235

Table 3.2 Neutron Temperature

ENRICHMENT(wt %)	TEMPERATURE(°C)
0.71	241.0
1.0	249.8
1.5	261.5
2.0	272.3
3.0	284.3
6.0	291.9

where I_0 is a zero order Bessel function of r and κ , a is the fuel pellet outer radius, and κ , β and λ are constants that vary with burnup. Since the ratio of power distribution in the CE-HAMMER code is an average value of each region, it is necessary to make a relationship which represents an average value within the boundary of each region as shown in Fig. 2.1. Hence, one can obtain the following relationship :

$$\bar{h}(\pi(r_2^2 - r_1^2)) = \int_{r_1}^{r_2} [h(0) I_0(\kappa r) + \beta \exp(\lambda(r-a))] 2\pi r dr \quad (3.2)$$

In order to make equation (3.2) more easily describable, it can be abbreviated as

$$\frac{\bar{h}(r_2^2 - r_1^2)}{2} = \int_{r_1}^{r_2} h(r) r dr \quad (3.3)$$

If we solve equation (3.3), we obtain the following results

$$\begin{aligned} \frac{\bar{h}(r_2^2 - r_1^2)}{2} = & h(0) \left\{ \frac{r_2 I_1(\kappa r_2) - r_1 I_1(\kappa r_1)}{\kappa} \right\} \\ & + \frac{h(0) \beta}{\lambda} \left\{ [r_2 \exp(\lambda(r_2 - a)) - r_1 \exp(\lambda(r_1 - a))] \right. \\ & \left. - \left[\frac{\exp(\lambda(r_2 - a)) - \exp(\lambda(r_1 - a))}{\lambda} \right] \right\} \quad (3.4) \end{aligned}$$

where

\bar{h} = average local fission rate of an arbitrary region,

$h(0)$ = the fission rate at the fuel centre,

$I_1(x)$ = modified Bessel function of the first kind.

The parameters, κ , β and λ , for the relative heat generation rate equation (3.4), were derived by fitting them to fission rate profiles calculated using the CE-HAMMER physics code. In order to obtain the values, $h(0)$, κ , β and λ , we used subroutine NL2INT⁽⁵⁾ to fit the curve of equation (3.4). The algorithm in NL2INT amounts to a variation on Newton's method in which part of the Hessian matrix is computed exactly and part is approximated by a secant (quasi-Newton) updating method. Once the iterations come sufficiently close to a local solution, they usually converge quite rapidly.

3.3 Application of the NEDAR Model Within a Fuel Performance Code

The flux depression resultant equations and neutron flux depression data-base have been incorporated as subroutines into the CANDU-PHWR type fuel performance analysis code,

KAFEPA⁽⁶⁾. At start of life, no plutonium is considered present so that the fuel pellet consists of stoichiometric UO_2 with a U-235 enrichment and dimensions supplied by the user.

When the input parameters of fuel enrichment, pellet diameter and final burnup are specified, multi-variate-interpolation routines obtain the values of κ , β and λ as a function of burnup for the particular case, and store these in the arrays TKS, TBS and TLS respectively into KAFEPA code. The values for κ , β and λ are then obtained at each history point (burnup step) by another 1-dimensional interpolation from the data stored in the arrays of TKS, TBS and TLS.

4. Results and Discussion

The predictions for radial power profile by KAFEPA incorporated with NEDAR model were compared with those of ELESIM code. Also, the predictions for fuel behavior in-reactor by KAFEPA and ELESIM codes were compared with the experiments indirectly.

The NEDAR model's predictions of radial power profile have been investigated for several cases of pellet conditions, enrichments, burnup and diameters. Figures 4.1 and 4.2 show the differences in the radial power profile between the original ELESIM data and the present data for selected cases, the neutron flux depression by ELESIM is slightly higher than that of KAFEPA-NEDAR. And it appeared that the effect of plutonium buildup in natural fuel is relatively higher than that of higher enriched fuel.

The first case considered was an artificial example chosen to demonstrate the magnitude of the effect of an evolving radial power profile on the performance of a fuel rod. As shown in Figure 4.3, the differences of the centre temperature were approximately more than 50°C. The change in the propile as burnup proceeds is clearly substantial and would have a very significant effect on the

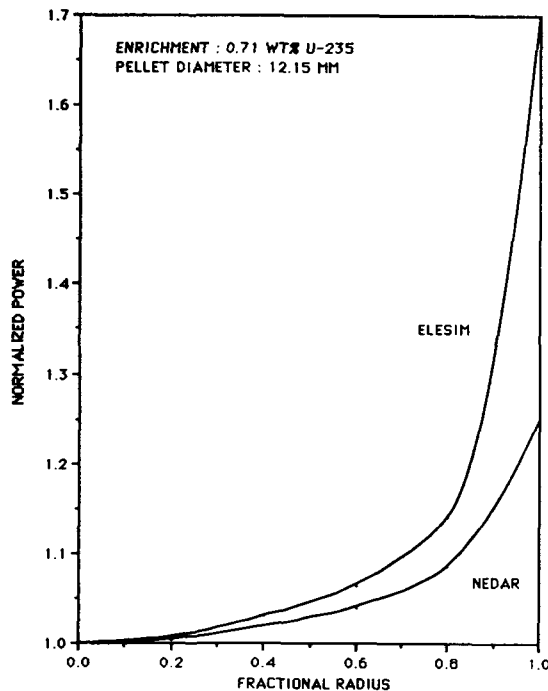


Fig. 4.1 Comparison of the Radial Power Profiles by ELESIM and KAFEP-NEDAR Codes : Burnup 5000 MWD/T, 0.71 wt % U-235

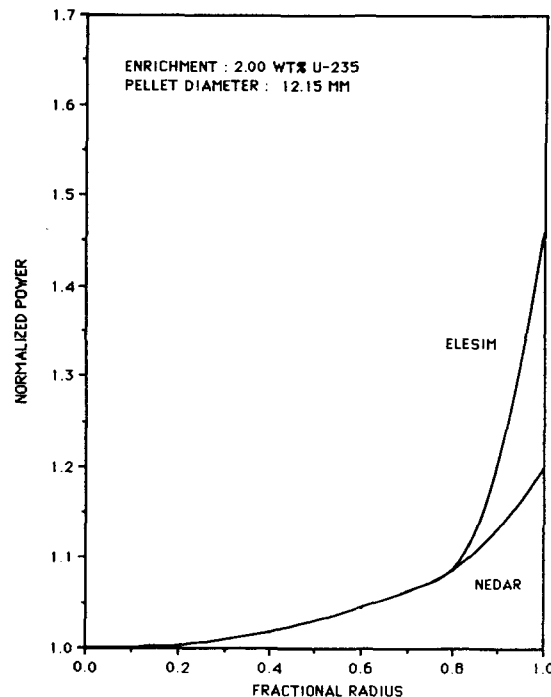


Fig. 4.2 Comparison of the Radial Power Profiles by ELESIM-WN and KAFEP-NEDAR Codes : Burnup 5000 MWD/T, 2.0 wt % U-235

performance of the fuel.

As shown in Figures 4.1 and 4.2, there are differences in radial profile in both cases. Also, Figures 4.4 to 4.6 show the differences in each parameter (κ , β , λ) between original ELESIM data and present data. There are differences in magnitude in every case. Occasionally, significant differences between the original ELESIM data and the present data exist. No formal record exists of the original assumptions made or techniques used in generating the original flux depression values used in ELESIM.

Table 4.1 and Figure 4.7 show that the predictions of the fission gas release by KAFEP-NEDAR are agree with the experiments slightly better than those of ELESIM. In case of KAFEP-NEDAR, the correlation coefficient of predictions is 0.9557, the slope is 1.227 and the inter-

cept is -4.603. While, in the case of ELESIM, the correlation coefficient of predictions is 0.9499, the slope is 1.268 and intercept is -5.737.

5. Conclusions

The thermal neutron flux profile in a fuel pellet is the solution of the resulting diffusion equations which are solved in terms of Bessel functions, I and K , and exponential function. Neutron flux depression tables for use in fuel performance analysis codes, such as KAFEP, were developed for fuel element diameters from 8.0 -19.5 mm, for the burnups up to 840 MWh/kg U (35 GWD/T) and for enrichments from 0.71 to 6 wt % U-235 in this work.

The neglect of changes in the radial power profile has been shown to lead to serious errors (of

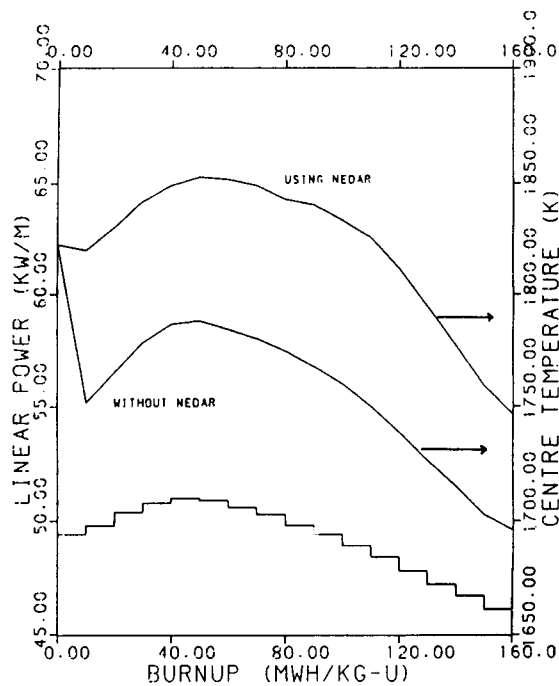


Fig. 4.3 Comparison of the Centre Temperatures As Predicted by ELESIM-WN and KAFEP-A-NEDAR Codes

50 °C or more) in the calculation of the fuel centre temperatures in fuel. The change in the profile as burnup proceeds is clearly substantial and would have a very significant effect on the performance of the fuel.

The predictions of the fission gas release by KAFEP-A-NEDAR are in slightly better agreement with the experiments than those of ELESIM. In the case of KAFEP-A-NEDAR, correlation coefficient of the predictions is 0.9557, while that value of ELESIM is 0.9499. The NEDAR model described in this paper has been shown to provide an effective, reliable and accurate method for determining radial power profiles in CANDU-PHWR fuel rods without incurring a significant increase in computing time. Also, KAFEP-A-NEDAR code is able to be used in long range of burnup, until 840 MWh/kgU.

The methodologies developed in this paper can be applied in the fuel of other reactor type. But, in this case, it is necessary to develop a neutron depression data table for the reactor type.

Table 4.1 Verification of Nedar Model by Comparing with Experiments

TEST ELEMENT	BURNUP MWh/kgU	FISSION	GAS RELEASE(%)	
		MEASURED	ELESIM	KAFEP-A-N
PICKERING-09794C	226	10.1-10.9	5.22	5.59
PICKERING-1022C	224	7.6-9.3	2.91	3.81
DFA(AECL-1676)	9.5	4.95	4.6	4.89
DFB(AECL-1676)	12.9	17.9	16.78	18.83
DFD(AECL-1676)	15.8	33.0	30.18	30.80
DFE(AECL-1676)	19.1	40.1	50.03	47.42
DFH(AECL-1676)	15.9	32.6	43.95	43.59
NR BDL-402	223	25.5-26.1	16.64	17.04
HZE(AECL-6585)	133	29.3	36.4	35.78
HZF(AECL-6585)	177.3	27.8	29.04	28.92
HZD(AECL-6585)	122.5	25.4	27.74	27.45
HZB(AECL-6585)	154.7	21.7	18.38	21.51
HZH(AECL-6585)	37.8	1.0	0.36	0.36
HZC(AECL-6585)	158.5	23.4	21.72	21.73
AGM NO. 7	201.3	7.29	2.71	3.12

NOTE : KAFEP-A-N stand for a ELESIM code with NADER model

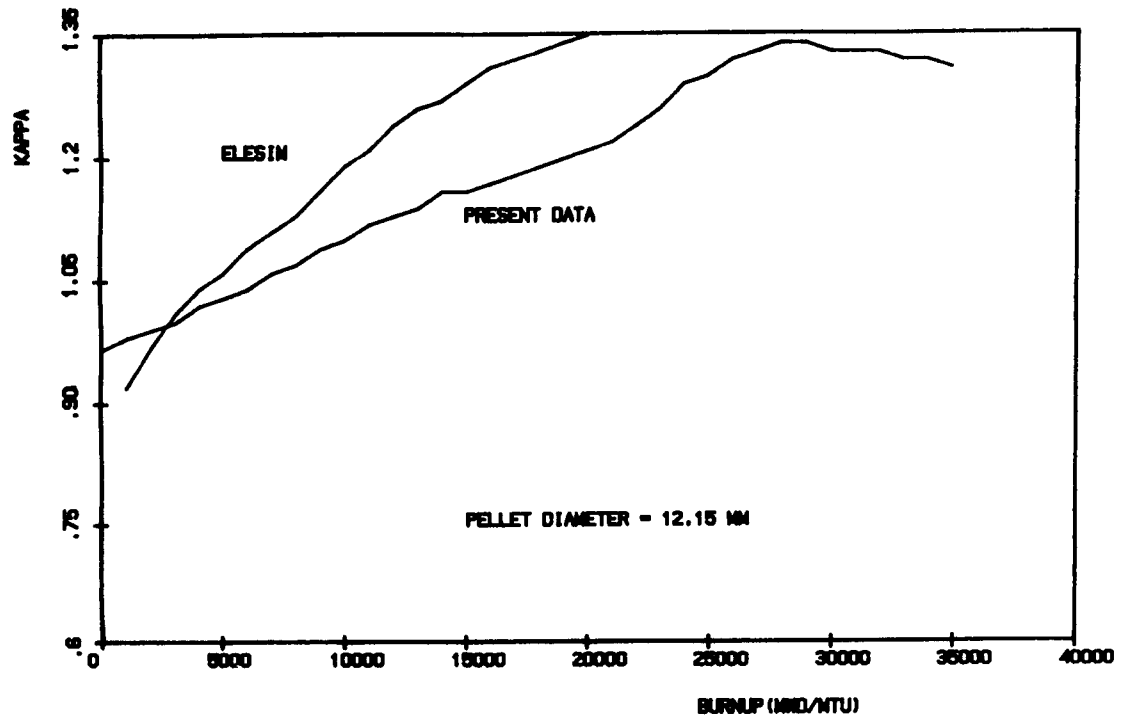


Fig. 4.4 Comparison of KAPPA As Predicted by KAFEPa-NEDAR and ELESIM for Pellet Diameter 12.15 mm, 0.71 wt % U-235

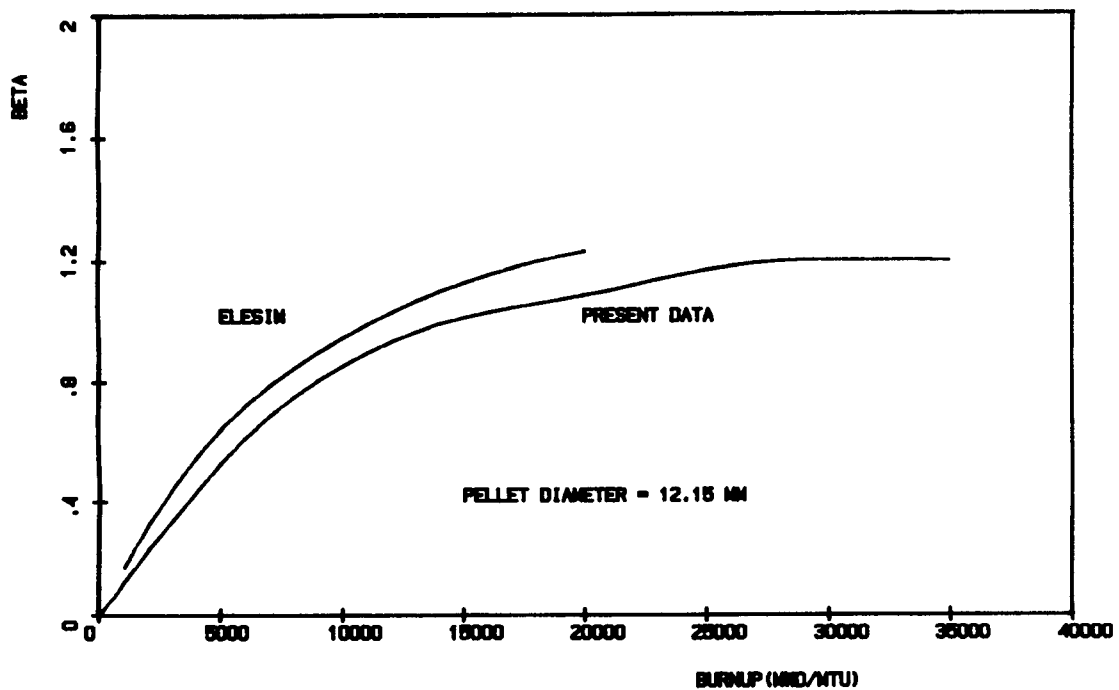


Fig. 4.5 Comparison of BETA Predicted by KAFEPa-NEDAR and ELESIM for Pellet Diameter 12.15 mm, 0.71 wt % U-235

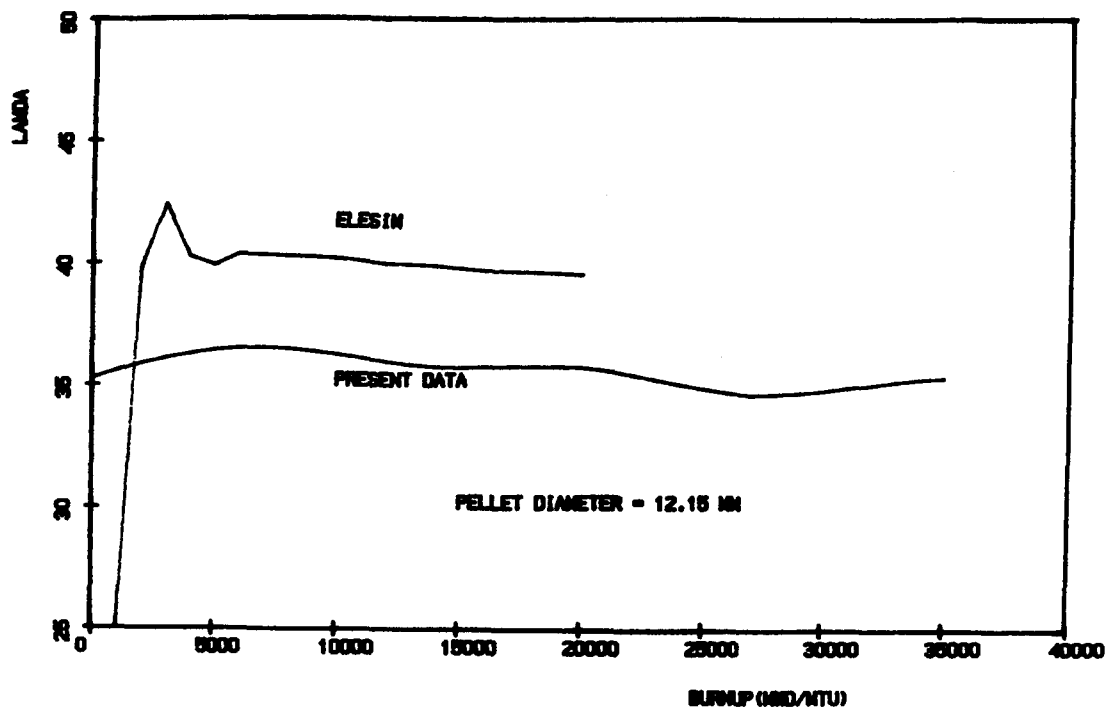


Fig. 4.6 Comparison of LAMDA Predicted by KAFEPa-NEDAR and ELESIM for Pellet Diameter 12.15 mm, 0.71 wt % U-235

References

1. M.J. Notley and I.J. Hastings, "A Microstructure-Dependent Model for Fission Product Gas Release and Swelling in UO_2 Fuel", Nuclear Engineering and Design, Vol.56, 163 (Mar. 1980).
2. J. WEISMAN, "Elements of Nuclear Reactor Design", ELSEVIER SCIENTIFIC PUBLISHING COMPANY AMSTERDAM-OXFORD-NEW YORK,(1977).
3. H. CARLSEN and D.N. SAH, "Radial Concentration and Effect on Temperature of Plutonium Formed in UO_2 During Irradiation", Nuclear Tech., VOL. 55, (Dec.1981).
4. U. Hesse, "Verification of the OREST (HAMMER-ORIGEN) Depletion Program System Using Post-Irradiation Analyses of Fuel Assemblies 168, 170, 171 and 176 from the Obrigheim Reactor", ORNL/TR-88/20, P. 1-32,(May 1984).
5. J.E. DENNIS, DAVID M. GAY AND ROY E. WELSCH, "Algorithm 573 NL2SOL-An Adaptive Nonlinear Least-Squares Algorithm (E4)", ACM Transactions on Mathematical Software, Vol.7,No.3, (Sep. 1981).
6. Ho Chun Suk, Woan Hwang et al, "The Development of KAFEPa Code", KAERI, (May 1985).
7. H.C. Suk, W. Hwang, and K.S.Sim, "KAFEPa : A Computer Code for CANDU-PHWR Fuel Performance Analysis under Reactor Normal Operating Condition", Journal of the Korean Nuclear Society, Vol.19, No.3, (Sep. 1987).
8. J.A.L Robertson, A.M. Ross, M.J.F. Notley and J.R. MacEwan, "Temperature Distribution in UO_2 Fuel Elements", Journal of Nuclear Mats.

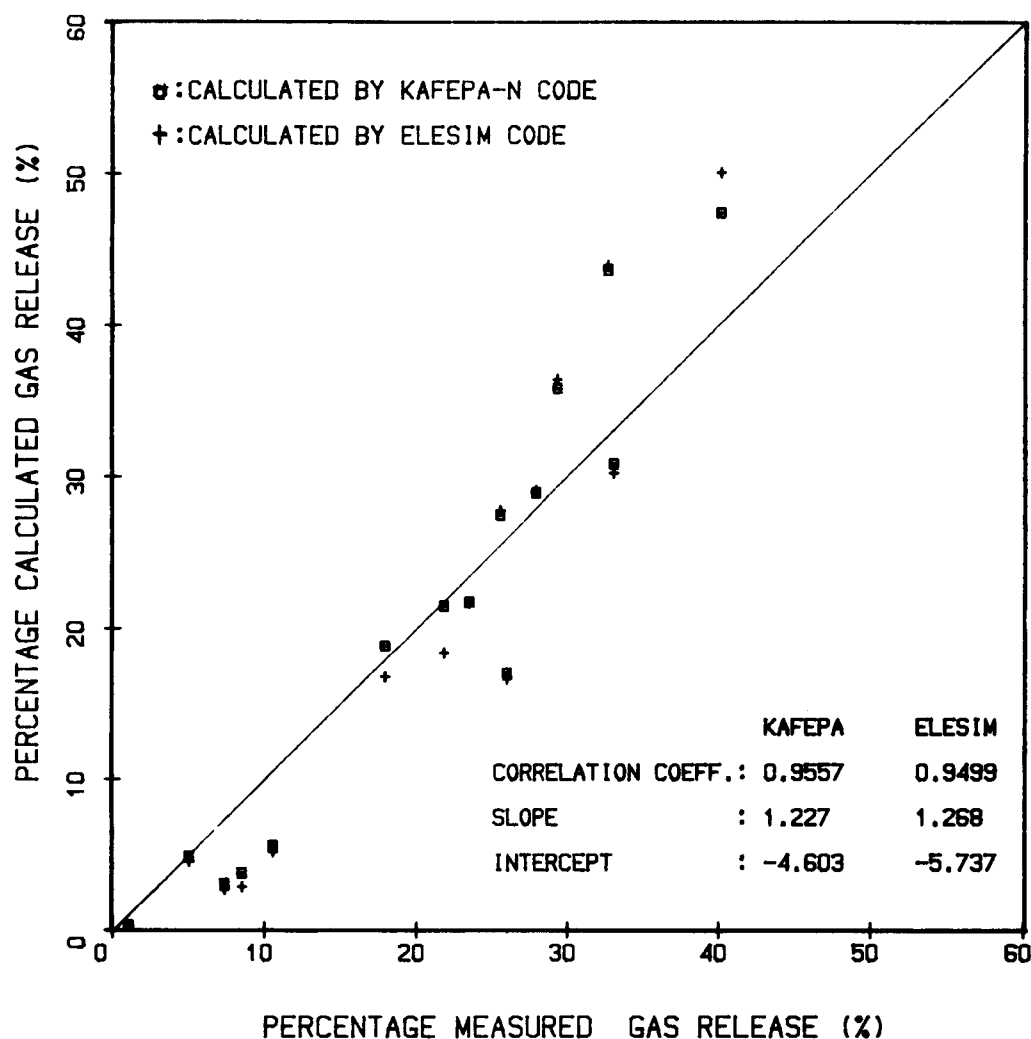


Fig. 4.7 Calculated versus Measured Gas Release from CANDU Fuel Elements

- 7, No.3, p 225-262, (1962).
9. Hellstrand E., "Measurement of the Effective Resonance Integral in Uranium Metal and Oxide in Different Geometries", Jour. App. Phys., 28, 1493 (1957).
10. James J. Duderstadt, Louis J. Hamilton, "Nuclear Reactor Analysis", Department of Nuclear Engineering, University of Michigan, (1976).
11. Raymond L. Murray, "Introduction to Nuclear Engineering", PRENTICE HALL INC., (1954).
12. George I. Bell and Samuel Glasstone, "Nuclear Reactor Theory", Van Nostrand Reinhold Company, (1970).
13. G.J. Phillips and J. Griffiths, "LATREP Users Manual", AECL-3857, (September 1971).
14. R.F. Coveyon, R.R. Bate and R.K. Qsbom, ORNL-1958 (1955).